Received: 26 September 2023 | Revised: 8 February 2024 | Accepted: 22 April 2024

DOI: 10.1111/jocd.16361

JCD Journal of Cosmetic Dermatology WILEY

ORIGINAL ARTICLE

Correction of age-related changes in the skin at the dermal and subdermal level using radiofrequency macroneedling therapy

Elena Flegontova MD, PhD[1,2] | Michael Kreindel PhD[3] | Neil M. Vranis MD[4,5] | R. Stephen Mulholland MD[6]

[1]Moscow Clinical Hospital by Speransky, Moscow, Russia

[2]Laboratory Angiopharm Private Clinic, Moscow, Russia

[3]InMode Inc., Yokneam, Israel

[4]Division of Plastic Surgery, Department of Surgery, Cedars Sinai Hospital, Los Angeles, California, USA

[5]Private Practice, Ghavami Plastic Surgery, Beverly Hills, California, USA

[6]Private Practice, SpaMedica Plastic Surgery Center, Toronto, Ontario, Canada

Correspondence
R. Stephen Mulholland, Private Practice, SpaMedica Plastic Surgery Center, Toronto, ON, Canada.
Email: smulholland@drm2.com

Abstract

Background: The negative effects of skin aging are primarily related to the destruction of dermal architectural structure. More specifically, this includes changes in the spatial arrangement of collagen, elastin fibers, mucopolysaccharides, proteoglycans, and ground substances.

Aims: The purpose of this study is to investigate the histologic effects of dermal and subdermal tissue after a controlled single treatment with radiofrequency (RF) macroneedling. This therapy provides a controlled, localized, thermal effect on the dermis whereby triggering the body's own healing processes of extracellular matrix remodeling. Clinically benefits include skin tightening.

Methods: Biopsies were obtained for histologic evaluation from four patients ($n = 4$), 4 weeks after completing a single RF macroneedling facial treatment.

Results: Age-related changes of the dermal and subdermal architecture were observed at baseline. After treatment, all biopsies demonstrated an increase in epidermal cells, collagen, elastin, fibroblasts, vasculature, and a decrease in inflammatory cells.

Conclusions: The results of this histologic study confirm a significant "subsurfacing" thermal effect from the noncoagulative ascendant thermal injury. The obtained results characterize RF macroneedling therapy as an effective method for correcting age-related changes in facial skin.

KEYWORDS
age-related skin changes, bipolar radiofrequency, collagen fibers, macroneedling therapy, subdermal remodeling,

1 | INTRODUCTION

As humans age, there is a predictable change in the structure of our skin. Thinning of the epidermal layer is due to atrophic changes in keratinocytes, which leads to increased trans-epidermal water loss and increased skin dryness. In addition, the two main components of the extracellular matrix—collagen and elastin—which are responsible for tensile strength and elasticity of the skin, respectively, undergo significant changes during aging.[1] There is a decrease in the amount of collagen due to a reduction of its

Produced by a bipolar radiofrequency device (Morpheus8, InMode, Lake Forest, CA).

synthesis. Collagen also becomes less functional due to an increase in structural fragmentation, which is presumably associated with the increased expression of matrix metalloproteinases (MMP) found in aging skin.[2]

Currently, about 28 distinct types of collagen have been described, which are encoded by more than 40 genes. Type I collagen (80%–90% of all skin collagen) and type III collagen are predominantly found in the skin. The relative amount of type III collagen increases significantly during the initial phase of wound healing. This has been observed after fractional CO_2 or radiofrequency epidermal-dermal ablative resurfacing treatments that activate the neo-collagenases cellular wound healing pathway. Type IV collagen forms a flat network of collagen fibers at the border of the epidermis and dermis responsible for maintaining integrity of the basement membrane (basal laminae). Collagen type V is combined in fibrils with collagen types I and III. It helps to regulate the diameter of the fibers. An important function is performed by type VII collagen, the main component of anchoring fibrils in order to provide adhesion between the epidermis and the underlying dermis.[3] Anchoring fibrils protect the skin from excessive stretching.

Elastin is an inert protein produced at an early age, so, there is virtually no new elastin formation during a human's lifetime. Any changes in elastin fibers that occur with aging tend to be permanent,[4,5] since the half-life of elastin is approximately 70 years. Consequently, only a minimal amount of this protein is synthesized during one's lifetime given the slow process of elastin genesis. It is estimated that only about 1% of elastin peptides are renewed per decade.[6] However, the fate of elastin is similar to all other types of protein found in humans—with age elastin is damaged and degraded.[7] Due to the extremely slow innate regeneration process, the degradation of elastin fibers is a practically irreversible and irreparable.[8] The increased activity of proteases associated with aging in elastin-rich tissues leads to the degradation of elastin and, simultaneously the increase of calcium deposits creating calcification of the soft tissues.[9] Changes in the quality and quantity of elastin fibers dramatically affect the skin's function, appearance, and ultrastructure. This decrease in elasticity accounts for the clinical classic age-related changes such as wrinkles and laxity.

As a result of ultraviolet (UV) radiation, photodamage of the skin is a known consequence. In vivo and in vitro studies have shown that UV radiation activates the elastin promoter and qualitative/quantitative changes in elastin fibers occur with a massive deposition of thickened, tangled, and amorphous fibers (solar elastosis). Unfortunately, this phenomenon is also facilitated by the formation of free radicals, which stimulate the synthesis and accumulation of abnormal elastin fibers.[10] Controlled damage is one of the most potent stimuli to remodel the dermal layer, thus, various technologies that harness this concept have been developed and applied in aesthetic medicine. In recent years, the delivery of thermal energy through high frequency oscillating, electrical current (radiofrequency energy) devices has become among one of the most popular.

1.1 | The use of the radiofrequency (RF) current in aesthetic medicine

Radiofrequency (RF) electric current was first used for medical purposes in 1926. During an operation, Dr. Harvey Williams Cushing used an electrosurgical generator developed by Dr. William Bovie to coagulate tissues. Since then, RF electric current has routinely been used in all surgical specialties as an ablative instrument. More recently, alternating RF electric current has found broader application in aesthetic medicine. When applied, the RF current causes vibrations of tissue molecules with a frequency of 1 000 000 Hz/s. As a result of micro-oscillations of tissue molecules, intermolecular, and intramolecular motion, kinetic energy is generated. This becomes converted into thermal energy. Heating of tissues at high temperatures can be ablative and coagulative, but, at a lower temperature it is nonablative. When applied at lower temperatures, thermal stimulation induces inflammation triggering neo-collagenesis and neo-elastogenesis. The main objective of this approach is to establish a dose–response thermal curve to safely heat targeted structures while mitigating the risk of irreversible thermal injury.[11]

Over the past 15 years, RF technology has undergone significant evolution. By changing the configuration and size of the electrodes and fractionating the delivery, one can control the energy density and, as a result can achieve the desired clinical effects while minimizing the risks of thermal injury.

Depending on the configuration of the electrodes, there are several main types of RF devices:

- Monopolar devices: energy is delivered through one active electrode with a relatively small contact surface, which is superimposed on the targeted area. The passive electrode, which is much larger than the active one is located at a certain distance from the treatment area. Monopolar systems affect the dermis and subcutaneous fat almost equally. With such a large radius, it is difficult to control the temperature and exposure level, thus, the risk of thermal damage is higher.
- Bipolar devices: these consist of two electrodes with different polarities ("+" and "−"). The advantage of bipolar systems is that the thermal effect is limited within the zone between the two electrodes. Therefore, when the electrodes come in contact with the skin's surface, the affected layers include the epidermis and partially the dermis, while the subcutaneous layer can be selectively targeted as needed.
- Multipolar devices: have more than two electrodes in the operating handpiece that change their polarity during exposure. At any given time, there are two bipolar electrodes activated. The continuous modification in trajectory and direction of the electric current between alternating electrodes reduce the risk of burns and provides uniform heating of the soft tissue under the handpiece.[12]

Most technologies that deliver controlled thermal damage aesthetic medicine target the dermal layer. However, if the energy

source is applied externally, the epidermal layer receives a significant amount of energy also. The epidermis is much more sensitive to heat; thus, thermal exposure of the epidermis entails an increased risk of complications and requires downtime.

Obstacles often serve as a stimulus to innovation and technologic advancement. In the process of creating a device for precise and targeted RF energy delivery, radiofrequency microneedling technology was born: the needles were modified to become electrodes. In this case, the RF impact depends on the needle electrode length and their coating. Furthermore, the concept of Macro-RF needling, or using longer, more powerful, monopolar, coated electrode-pins to penetrate more deeply to the subdermal adipose tissue was the next generation of innovation.

These new technologies made it possible to focus fractional, coated electrode-macro-needle RF energy on another target—the subcutaneous fat layer. Therefore, in addition to treating the dermis, there is a synergistic effect on deeper soft tissue contraction, adipolysis, and overall tightening.[13] The subcutaneous fat layer is divided into lobules, separated by connective tissue septa forming the fibro-septal network (FSN) designed to connect the dermis securely to the underlying muscle fascia (Figure 1).

Each of the needle electrodes of the applicator are positively charged and emit RF current only from the tip. The operator can precisely control depth of penetration into the dermis and/or adipose tissue. Maximum depths on the Morpheus8 device (InMode, Lake Forest, CA) are 8 mm for coagulation/heating and 7 mm for ablation. At these maximum depths the delivery of energy targets the subcutaneous adipose tissue as well the FSN. Importantly, a built-in safety mechanism ensures that the tips of each electrode-pin are positively charged while the negative return electrodes remain on the surface. Since the negative electrodes cover a much larger surface area, the superficial thermal zone of injury is minimized allowing for a greater amount of deeper energy to be delivered. For each fractional electrode needle, the RF emission produces three zones of thermal injury in the nearby deep tissues—an ablation zone, a zone of reversible coagulation (when introduced into the fat layer, these two zones cause a shortening and contraction of the FSN) and finally, a large zone of noncoagulative, nonablative tissue heating created by the RF current flowing from deep inside the adipose tissue up to the negative electrodes on the surface of the skin. (Figure 2).

The ablation zone is created when tissue is heated beyond 100°C and can range from 100 to 500 microns in diameter, while the reversible coagulation zone is created when the temperatures reach 60–85°C and can be 600–800 microns in diameter. After ablative damage to adipose tissue, the RF current flows back to the negative return electrode on the skin surface, gently heating the dermis and epidermis. This nonablative, coagulative, and noncoagulative thermal stimulation is what we term "fractional RF sub-surface remodeling." It should be thought of as an "upside down cone" caused by the bipolar RF flowing back to the negative electrode from the internal, positively charged ablative positively charged electrode to the larger surface area, negatively charged plate. This nonablative, coagulative, and noncoagulative heating serves as the thermal stimulation for the formation of new collagen and elastin.[11,14] The heating of the skin surface does not exceed 42°C which has been found to be the threshold for irreversible epidermal thermal injury.

After RF exposure, an immediate shortening of the FSN fibers occurs. The horizontal, oblique, and vertical connective tissue fibers simultaneously contract to achieve a three-dimensional shrink-wrap effect. Additionally, soft tissue contraction and skin thickening can reach 40%–70% (30%–40% due to FSN + 20%–30% secondary to dermal contraction). The thermal energy delivered reduces thickness of adipose tissues affecting external contours in addition to reducing/eliminating overlying wrinkles, folds, scars (including post-acne scaring), uneven skin texture, pores and stretch marks.

The purpose of this study is to investigate the histologic effects of dermal and subdermal tissue after a controlled single treatment with RF microneedling. We anticipate that there will be histologic

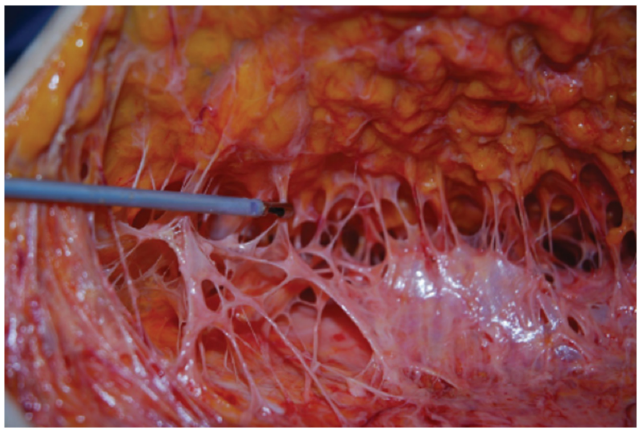

FIGURE 1 Fibers of the fibro-septal network (FSN) of adipose tissue.

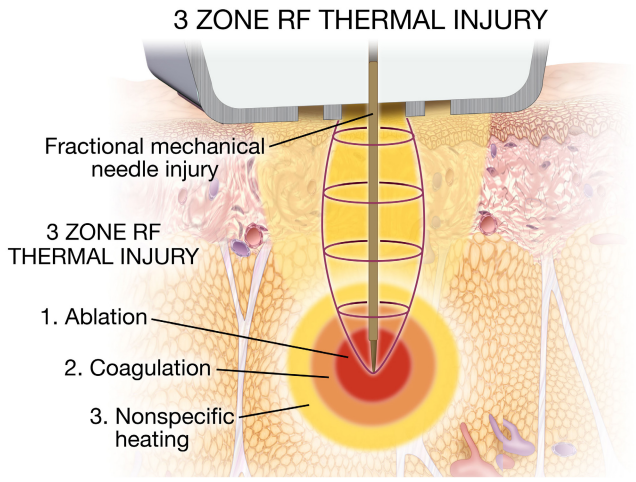

FIGURE 2 Three different thermal zones of injury produced by the Morpheus8 device (InMode, Lake Forest, CA).

evidence that correlates with the clinical observations of skin tightening and skin thickening.

2 | MATERIALS/METHODS

Each needle electrode of the Morpheus8 device (InMode, Lake Forest, CA) has a gold coating except for the distal 500 microns, where the RF energy is emitted. The tip of each electrode-needle is positively charged, and the larger, flat, planar designed negative side-rail electrodes stay on the surface of the skin. The RF energy flows from the tips of the microneedles to external electrodes set on the skin surface. The patented pulse of RF energy ablates and coagulates the subdermal adipose tissue and more importantly, shortens the FSN's horizontal, oblique, and vertical connective tissue fibers. (Figure 3). The pulse duration has been calibrated by the manufacturer to account for thermal relaxation time of the dermis and subcutaneous tissue in order to maximize energy delivery and minimize risk of irreversible thermal injury.

Ablative and coagulative injury was meticulously delivered to soft tissues at the various subcutaneous levels, with noncoagulative, nonablative thermal stimulation of the reticular and papillary dermis from the "bottom up", or "Fractional RF Sub-Surfacing" while protecting the epidermis from thermal damage. The settings were consistent for all patients in this study to minimize variables and maintain consistency of treatment parameters.

2.1 | Post-treatment reduction of age-related skin changes and their morphological characteristics

Patients volunteered for the study and consent was obtained in accordance with the Declaration of Helsinki. To assess changes in skin structure after Morpheus8 (InMode, Lake Forest, CA) RF macroneedling therapy, we conducted a clinical study involving subjects of the following two age groups:

- Group 1: 35–40 years old (subjects 1–3);
- Group 2: > 40 years old (subject 4, 69 years old).

The facial area of the participants was treated with the facial applicator using the following single pass parameters: 2 mm depth and 22 mj/pin of energy. This was selected because all patients were Fitzpatrick type 2 and 3 without excess subcutaneous adiposity.

Before and after the procedure, eight biopsies from the treated area were obtained from subjects. All biopsies were taken 28 days after the procedure at the 4-week follow-up visit. During the histological examination, the following parameters were evaluated:

(i) The thickness of skin layers;
(ii) Number of fibroblasts and inflammatory cells (lymphocytes and macrophages);
(iii) Surface area of vessels in the papillary and outer layers of the reticular dermis;
(iv) The density of collagen and elastin fibers in the dermis, as well as the degree of fragmentation of elastin fibers (analyzed by semi-quantitative scoring method on a 5-point scale, where 0—none, 4—maximum intensity).

The pathologist used the following collagen degradation scale to determine the "Fiber Score." Score = 0: Collagen bundles are not visualized, they are disintegrated into individual fibers. Score = 1: Bundles are loosely arranged, fibers within are moderately loosened. Score = 2: Bundles are arranged with moderate density, there are areas of loosening of individual fibers. Score = 3: Bundles are arranged closely to each other, there are small areas of loosening of individual fibers. Score = 4: Bundles are densely arranged, fibers are tightly packed, parallel to each other. Five visual fields were analyzed in each sample, and about 50 measurements were made for each parameter.

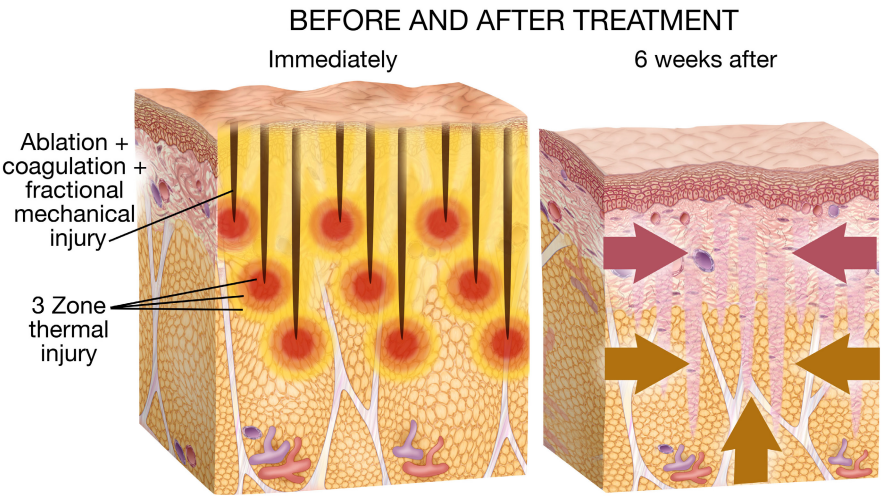

FIGURE 3 Multiple passes of Morpheus8 (InMode, Lake Forest, CA) at different depths results in horizontal and vertical fractional remodeling of adipose tissue and FSN. This also leads to dermal remodeling for optimal skin tightening, contouring, and soft tissue contraction.

3 | RESULTS

3.1 | Comparison of the morphological characteristics of the skin of subjects before the fractionated RF macroneedling procedure

Table 1 presents data as mean values ± standard error of the mean or as median values and interquartile range (in the case of score evaluation). At baseline, subject 4 (69 years old) had a lower epidermal thickness (28.2% less) compared to subjects aged 39–40 years, while the thickness of the dermal layers was unchanged (Figures 4–9).

The older aged individual demonstrated a decrease in the average number of epidermal cells (38.4% less), fibroblasts (29.5% less), and inflammatory cells (73.7% less). Age-related changes in the vascular area were also observed. A decrease in the density of collagen fibers (33.3% less) and an increase in the degree of fragmentation of elastin fibers (33.3% more) were visualized on histology.

TABLE 1 Morphometric analysis of morphological features in skin biopsies of subjects of different ages before and after treatment.

	Subjects 1–3 (35–40 y.o.)		Subject 4 (69 y.o)	
Morphological signs	**Before treatment**	**After treatment**	**Before treatment**	**After treatment**
Layer thickness (μm)				
Epidermis	58.2 ± 2.8	56.9 ± 2.2	41.8 ± 2.5	35.7 ± 1.2
Papillary dermis	87.3 ± 3.2	98.4 ± 3.3	80.9 ± 3.8	61.03 ± 4.5
Reticular layer of the dermis (outer part)	302.3 ± 5.6	318.2 ± 9.6	321.4 ± 9.2	314.8 ± 13.5
Cellular composition (pcs)				
Epidermal cells	150.4 ± 6.1	162.6 ± 7.8	95.7 ± 2.3	91 ± 5.1
Fibroblasts	117 ± 10.4	141.7 ± 7.6	82.5 ± 3.8	85.8 ± 3.5
Inflammatory cells	67.7 ± 7.6	51.8 ± 6.8	17.8 ± 4.6	10.2 ± 1.5
Vessels (μm^2)				
Vessels surface area	3064 ± 538.3	5597 ± 1089	2349 ± 680.4	3996 ± 739.1
Fiber (score)				
The density of collagen fibers	3 (3; 3)	4 (3; 4)	2	2
The density of elastin fibers	2 (2; 2)	3 (2; 3)	2	4
Fragmentation of elastin fibers	2 (2; 3)	1 (1; 1)	3	1

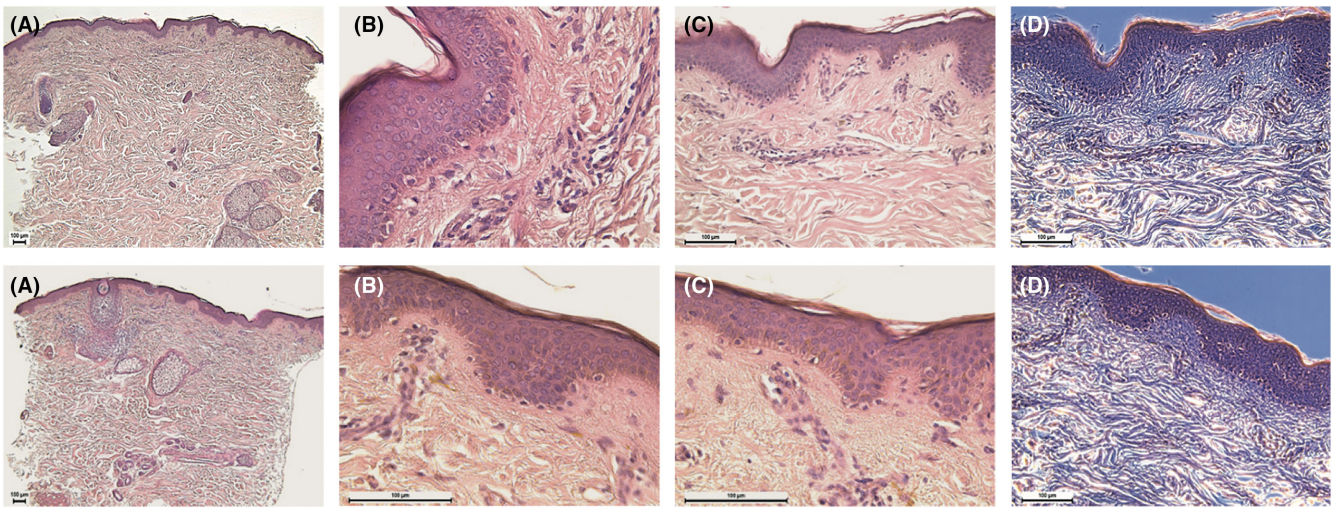

FIGURE 4 Top Row: Histological structure of the skin biopsy of subject one before treatment, stained with hematoxylin–eosin: (A) general view of the epidermis, reticular, and papillary dermis; (B) moderate dystrophic changes in the cells of the epidermis and a slight perivascular inflammatory infiltration in the papillary dermis; (C) the structure of the papillary and reticular layers of the dermis; (D) thin and loose fibers in the papillary layer and thicker bundles of fibers in the reticular layer. Bottom Row: Histological structure of the skin biopsy of subject one after the procedure, stained with hematoxylin–eosin: (A) general view of the epidermis, reticular, and papillary dermis; (B) Weak dystrophic changes in the cells of the epidermis and a slight perivascular inflammatory infiltration in the papillary dermis; (C) the structure of the papillary and reticular layers of the dermis; (D) a denser arrangement of thin fibers in the papillary layer.

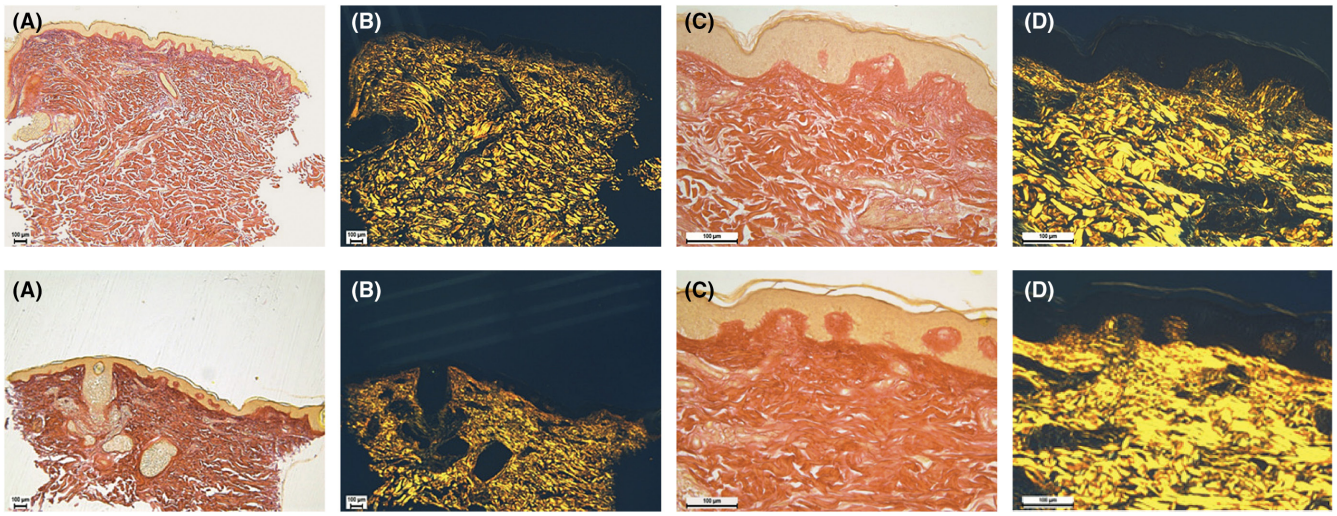

FIGURE 5 Top Row: Histological structure of collagen fibers in the skin biopsy of subject one before treatment, stained with picrosirius red: (A) collagen fibers of the reticular and papillary dermis are stained red; (B) collagen fibers give yellow anisotropy; (C) thinner and looser collagen fibers are located in the papillary dermis, and thicker bundles of collagen fibers are visible in the reticular layer; (D) collagen fibers give yellow anisotropy of varying intensity depending on the thickness and density of collagen fibers in different layers of the dermis. Bottom Row: Histological structure of collagen fibers in the skin biopsy of subject one after the procedure, stained with picrosirius red: (A) collagen fibers of the reticular and papillary dermis are stained red; (B) collagen fibers give yellow anisotropy; (C) thinner and looser collagen fibers are located in the papillary dermis, and thicker bundles of collagen fibers are visible in the reticular layer; (D) collagen fibers give yellow anisotropy of varying intensity depending on the thickness and density of collagen fibers in different layers of the dermis.

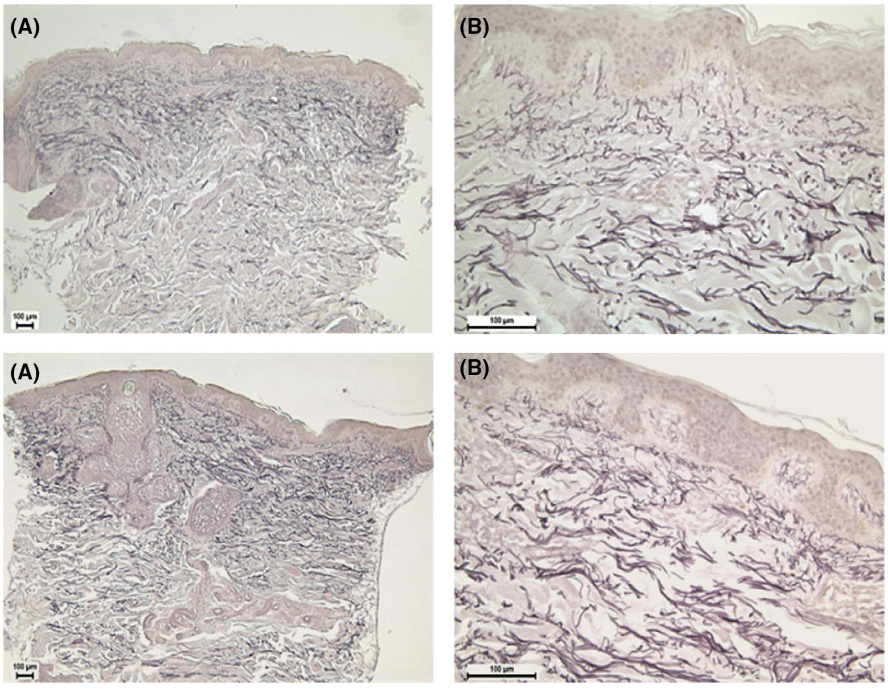

FIGURE 6 Top Row: Histological structure of elastin fibers in the skin biopsy of subject one at baseline, pretreatment, stained with orcein: (A) collagen fibers of the reticular and papillary dermis are stained black; (B) thinner and shorter elastin fibers are seen in the papillary dermis and thicker and loosely located elastic fibers are seen in the reticular layer. Bottom Row: Histological structure of elastin fibers in the skin biopsy of subject one after the procedure, stained with orcein: (A) collagen fibers of the reticular and papillary dermis are stained black; (B) an increase in the content of elastin fibers in the layers of the dermis, their longitudinal orientation in the reticular layer.

3.2 | Comparison of the morphological characteristics of the skin of subjects after the Morpheus8 procedure

After the procedure, the younger cohort (Group 1) representing subjects 1–3, displayed a an increase in the number of epidermal cells (by 8.1%) and fibroblasts (by 21.1%) as well as a decrease in the number of inflammatory cells (by 23.5%). In cohort 2, subject 4, after treatment, a decline in the number of inflammatory cells (by 42.7%) was observed.

In all subjects, regardless of age, a significant increase in the area of the vessels was observed: in the group of subjects 1–3, by 1.8 times, and in subject 4, by 1.7 times (Graph 1). In the group of younger subjects, 1–3, after the procedure, there was an increase

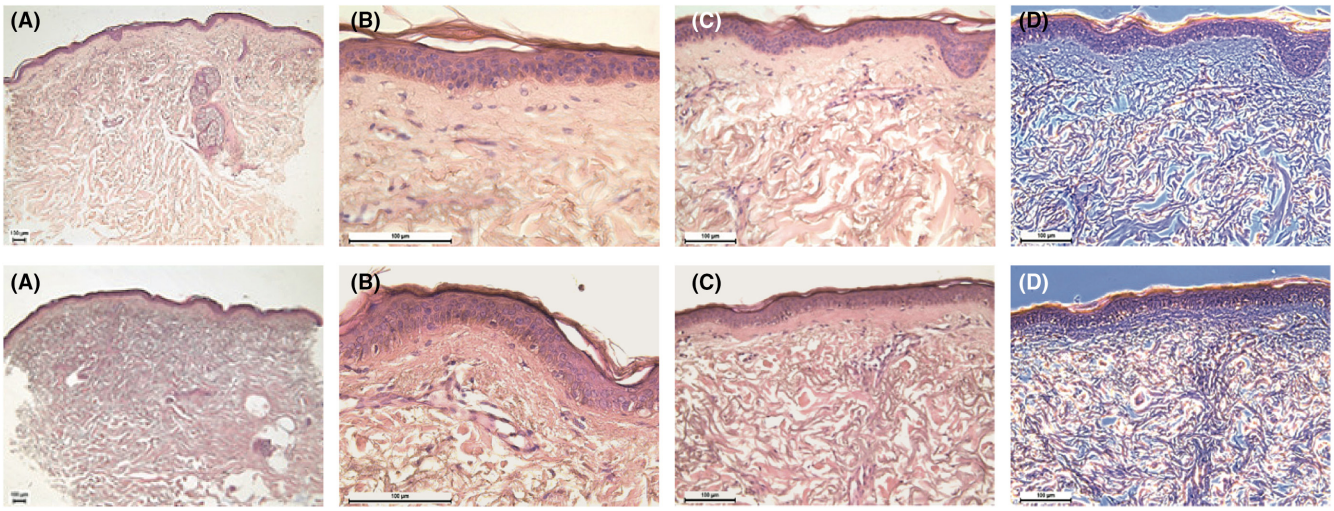

FIGURE 7 Top Row: Histological structure of the skin biopsy of subject four (69 years old) before the treatment, stained with hematoxylin–eosin: (A) general view of the epidermis, reticular, and papillary layers of the dermis; (B) thinned epidermis, thickened papillary dermis; (C) inadequate vascularization and moderate perivascular inflammatory infiltration in the dermis; (D) the same area with phase-contrast microscopy. Bottom Row: Histological structure of the skin biopsy of subject four after the procedure, stained with hematoxylin–eosin; (A) general view of the epidermis, reticular, and papillary layers of the dermis; (B) a thin layer of the epidermis and papillary layer, an increase in the content of blood vessels in the papillary layer; (C) the structure of the papillary and reticular layers of the dermis with increased range of blood vessels; (D) the same area with phase-contrast microscopy.

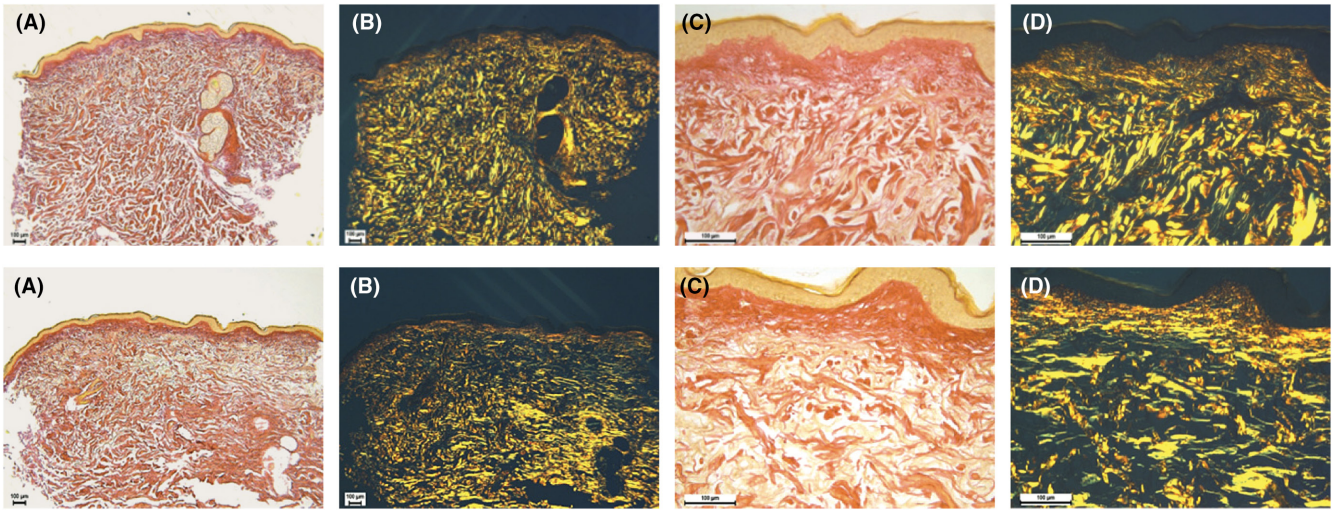

FIGURE 8 Top Row: Histological structure of collagen fibers in the skin biopsy of subject four (69 years old) before the procedure, stained with picrosirius red: (A) collagen fibers of the reticular and papillary dermis are stained red; (B) collagen fibers give yellow anisotropy; (C) dense arrangement of thin collagen fibers in the papillary dermis, loose structure of bundles of collagen fibers in the reticular layer; (D) collagen fibers give yellow anisotropy of varying intensity depending on the thickness and density of collagen fibers in different layers of the dermis. Bottom Row: Histological structure of collagen fibers in the skin biopsy of subject four (69 years old) after the procedure, stained with picrosirius red; (A) collagen fibers of the reticular and papillary layers of the dermis are stained red; (B) collagen fibers give yellow anisotropy; (C) increase in the content of collagen fibers in the papillary dermis; (D) increased anisotropy of collagen fibers in the layers of the dermis.

in the density of collagen (by 25%), elastin (by 33.3%) fibers and a decrease in the degree of fragmentation of elastin fibers (by two times) were observed. In subject 4, after treatment, there was an increase in the density of elastin fibers (2 times) and a decreasing degree of fragmentation (3 times).

4 | DISCUSSION

Recent research has validated the effects of the Morpheus8 (InMode, Lake Forest, CA) on the RF-induced FSN tightening and adipose-related soft tissue contraction which is significant. This

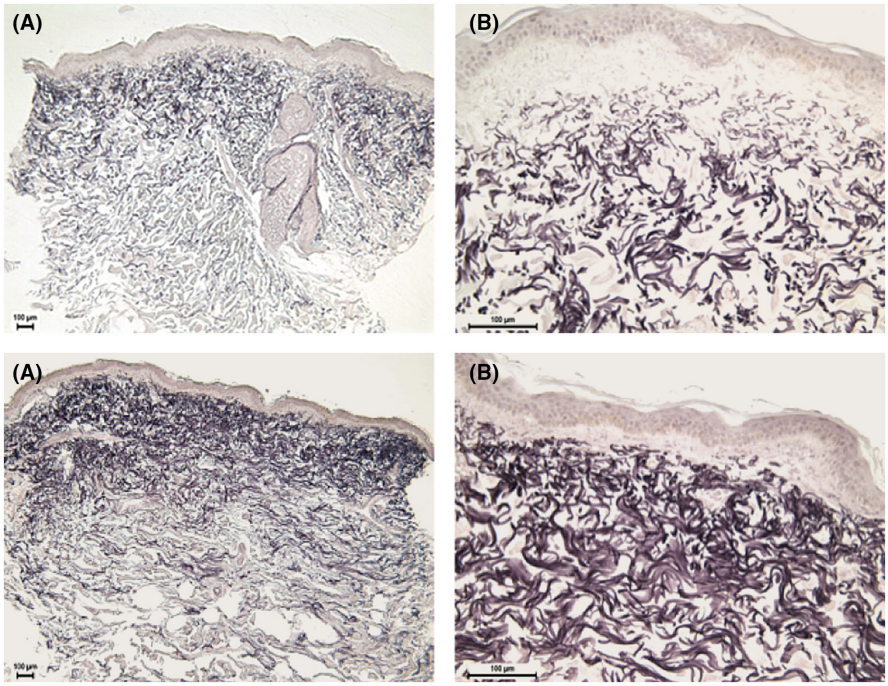

FIGURE 9 Top Row: Histological structure of elastin fibers in the skin biopsy of subject four (69 years old) in the initial state, stained with orcein; (A) collagen fibers of the reticular and papillary layers of the dermis are stained black; (B) hypoelastosis and fragmentation in the papillary dermis with evidence of hyperelastosis and fragmentation in the reticular dermis. Bottom Row: Histological structure of elastin fibers in the skin biopsy of subject four (69 years old) after treatment, stained with orcein; (A) collagen fibers of the reticular and papillary layers of the dermis are stained black; (B) hyperelastosis in the reticular layer of the dermis.

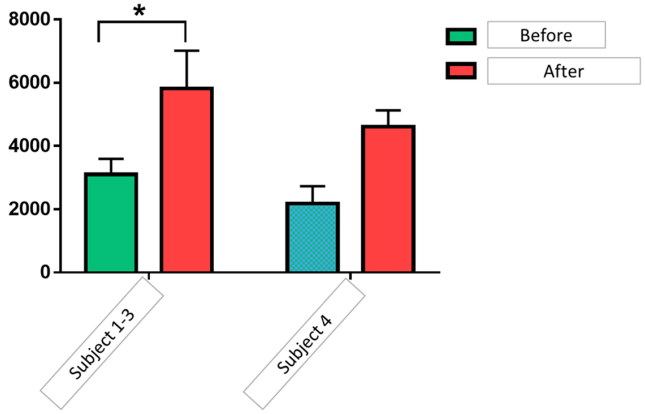

GRAPH 1 Change in the vascular area in subjects of both age groups after the Morpheus8 procedure. $P<0.05$.

focused on the dermal histologic effects of the novel adipose thermal ablation and coagulation. We found that, at baseline, in the initial state, the skin of subjects aged 35–40 was characterized by moderate dystrophic changes in the epidermis cells. In the papillary dermis, collagen fibers were primarily thin and loosely arranged, while elastin fibers were also light, sparse, and fragmented. Sometimes in the papillary layer, there were separate areas of noticeable fibers loosening with increased content of lymphocytes and macrophages, as well as foci of compaction and tissue homogenization (fibrosis and hyalinosis).

In the reticular dermis, collagen fibers formed bundles and were denser; elastin fibers were also thicker, often fragmented, and unevenly distributed. The cellular composition of the dermis was mainly represented by fibroblasts and a few vessels with moderate perivascular infiltration from lymphocytes and macrophages.

A month after RF treatment, dystrophic changes in epidermal cells were almost not detected. There were no areas of sharp loosening of the fibers, as well as foci of fibrosis and hyalinosis in the dermis. In the papillary dermis, the density of collagen fibers increased, elastin fibers were located more evenly, and their degree of fragmentation decreased. In the reticular layer, there was an increase in the content of collagen and elastin fibers with a simultaneous decrease in their fragmentation. The number of fibroblasts and vessels in the dermis increased, while the amount of lymph-macrophage infiltration was minimal.

In a skin biopsy of the older subject (69 years old), a pronounced thinning of the epidermis was observed before the procedure. In the thickened papillary dermis, thin collagen fibers were very densely packed, while significantly fewer elastin fibers (hypoelastosis) and their fragmentation were observed. In the reticular dermis, a loose arrangement of bundles of collagen fibers was noted. In the outer areas of the reticular layer, hyperelastosis was detected, and in deeper areas, the density of elastin fibers decreased, and fragmentation increased. The content of fibroblasts and vessels in the layers of the dermis was reduced while only few lymphocytes and macrophages were noted.

Most of these histological changes cannot be just attributed to the mechanical injury of the single pass microneedling as the increased vasculature in the reticular dermis, the notable neo-elastogenesis and reorganized and compacted papillary and reticular dermis have not been noted in published, nonthermal, microneedling papers. Thus, we postulate that the strong noncoagulative heating of the return RF traveling from the deep positive ablative and coagulative electrode up to the negative electrode created this “subsurfacing” or “upside down” thermal remodeling. This subsurfacing effect is not present with the typical RF microneedling design where the needles penetrating into the deep dermis or superficial adipose are alternating rows of positive and negatively charged bipolar electrodes. The

ablative and coagulative index for these RF microneedling bipolar arrays is small compared to the Morpheus8 (InMode, Lake Forest, CA), and there is no RF flow up to negative electrodes on the surface of the skin, which generates the reticular and papillary thermal effects.

It would be interesting to extend this study with additional subjects to achieve greater power to determine if these trends would persist. Additionally, it would be valuable to determine if a depth at 1 mm, would the "subsurfacing" effect be just as dramatic. It would also be of value to compare the subdermal and transdermal effects of Radiofrequency-Assisted Liposuction (RFAL) which involves AccuTite, FaceTite, and BodyTite (InMode, Lake Forest, CA).

After radiofrequency macroneedling therapy, the structure of the epidermis did not fundamentally change; the content of vessels and elastin fibers in the papillary layer increased. The most significant changes occurred in the reticular layer, with a strong predominance of densely located elastin fibers (hyperelastosis) over loosened collagen fibers. Thus, the radiofrequency microneedle therapy had a beneficial effect on the skin condition of subjects of different ages: a decrease in the severity of age-related changes and increased regenerative properties were observed. In order to maintain consistency in this case series, all patients were treated with a single pass at 2 mm depth and 22 mj/pin of energy. This mitigates confounding variables such as stacking pulses and multiple passes. Clinically, most patients will receive multiple passes and pulses at multiple depths. Thus, these changes are even more impressive when considering it is due to a single shot of RF delivered by the macroneedles in a given area.

In skin biopsies after the procedure, an increase in the number of epidermal cells, fibroblasts, and blood vessels was noted, the density of collagen and elastin fibers in the dermis layers increased, dystrophic changes in cells and inflammatory infiltration were minimal. It should be noted that in older subjects, the effectiveness of treatment was more pronounced due to the pronounced stimulation of elastogenesis in the reticular layer of the dermis.

5 | CONCLUSION

The Morpheus8 (InMode, Lake Forest, CA) device can deliver a deep and profound FSN and adipocyte ablative and coagulative injury resulting in FSN soft issue contraction and adipose destruction and liquification with the resulting soft tissue tightening and adipose reduction and contouring.[13] The results of this histologic study confirm a significant "subsurfacing" thermal effect from the noncoagulative ascendent thermal injury and. The obtained results characterize radiofrequency macroneedling (micro electrode) therapy as an effective method for correcting age-related changes in facial skin in subjects of different age groups. A study with a larger sample size is needed to confirm the statistical significance of the recorded changes in skin condition.

AUTHOR CONTRIBUTIONS

All authors have read and approved the final version of the manuscript. EF and MK were involved in study design, data collection and histologic analysis. RSM and NV were involved in writing and editing the manuscript.

FUNDING INFORMATION

The authors received no financial support for the research, authorship, and publication of this article.

CONFLICT OF INTEREST STATEMENT

Dr. Mulholland is a paid consultant and shareholder of InMode. Dr. Kreindel is the chief technology officer of InMode. Dr. Vranis and Dr. Flegontova have no disclosures.

DATA AVAILABILITY STATEMENT

The data that support the findings of this study are available from the corresponding author upon reasonable request.

ETHICS STATEMENT

All procedures were performed according to the standard of care at the time of service. Data was collected retrospectively and the patient data was immediately de-identified and essentially anonymous.

ORCID

Neil M. Vranis https://orcid.org/0000-0003-4015-5130

REFERENCES

1. Chambers ES, Vukmanovic-Stejic M. Skin barrier immunity and aging. *Immunology*. 2020;160(2):116-125.
2. Fligiel SE, Varani J, Datta SC, Kang S, Fisher GJ, Voorhees JJ. Collagen degradation in aged/photodamaged skin *in vivo* and after exposure to matrix metalloproteinase-1 in vitro. *J Invest Dermatol*. 2003;120:842-848.
3. Cao Q, Tartaglia G, Alexander M, et al. Collagen VII maintains proteostasis in dermal fibroblasts by scaffolding TANGO1 cargo. *Matrix Biol*. 2022;111:226-244.
4. Le Page A, Khalil A, Vermette P, et al. The role of elastin-derived peptides in human physiology and diseases. *Matrix Biol*. 2019;84:81-96.
5. Sugitani H, Hirano E, Knutsen RH, et al. Alternative splicing and tissue-specific elastin misassembly act as biological modifiers of human elastin gene frameshift mutations associated with dominant cutis laxa. *J Biol Chem*. 2012;287(26):22055-22067.
6. Halabi CM, Mecham RP. Elastin purification and solubilization. *Methods Cell Biol*. 2018;143:207-222.
7. Janig E, Haslbeck M, Aigelsreiter A, et al. Clusterin associates with altered elastic fibers in human photoaged skin and prevents elastin from ultraviolet-induced aggregation in vitro. *Am J Pathol*. 2007;171(5):1474-1482.
8. Robert L, Molinari J, Ravelojaona V, Andrès E, Robert AM. Age- and passage-dependent upregulation of fibroblast elastase-type endopeptidase activity. Role of advanced glycation endproducts, inhibition by fucose- and rhamnose-rich oligosaccharides. *Arch Gerontol Geriatr*. 2010;50:327-331.
9. Pierre A, Lemaire F, Meghraoui-Kheddar A, Audonnet S, Héry-Huynh S, Le Naour R. Impact of aging on inflammatory and immune responses during elastin peptide-induced murine emphysema. *Am J Physiol Lung Cell Mol Physiol*. 2019;316:L608-L620.
10. Kawaguchi Y, Tanaka H, Okada T, et al. Effect of reactive oxygen species on the elastin mRNA expression in cultured human dermal fibroblasts. *Free Radic Biol Med*. 1997;23:162-165.

11. Mulholland S. *The InMode Book* 2021. Marquis Publishing Inc, Montmagny, Quebec, Canada. https://prev.boomerangfx.com/the-inmode-book-3/
12. Gold M. Noninvasive skin tightening treatment. *J Clin Aesthet Dermatol*. 2015;8(6):14-18.
13. Dayan E, Chia C, Burns AJ, Theodorou S. Adjustable depth fractional radiofrequency combined with bipolar radiofrequency: a minimally invasive combination treatment for skin laxity. *Aesthet Surg J*. 2019;39(Suppl 3):S112-S119.
14. Kauvar ANB, Gershonowitz A. Clinical and histologic evaluation of a fractional radiofrequency treatment of wrinkles and skin texture with novel 1-mm long ultra-thin electrode pins. *Lasers Surg Med*. 2022;54:54-61.

How to cite this article: Flegontova E, Kreindel M, Vranis NM, Mulholland RS. Correction of age-related changes in the skin at the dermal and subdermal level using radiofrequency macroneedling therapy. *J Cosmet Dermatol*. 2024;00:1-10. doi:10.1111/jocd.16361